Growth and characterization of multiferroic $BiMnO_3$ thin films

Hyoungjeen Jeen, Guneeta Singh-Bhalla,[a] Patrick R. Mickel, Kristen Voigt, Chelsey Morien, Sefaattin Tongay,[b] A. F. Hebard, and Amlan Biswas[c]
Department of Physics, University of Florida, Gainesville, Florida 32611, USA

(Received 21 May 2010; accepted 22 January 2011; published online 5 April 2011)

We have grown epitaxial thin films of multiferroic $BiMnO_3$ using pulsed laser deposition. The films were grown on $SrTiO_3$ 001 substrates by ablating a Bi-rich target. Using x-ray diffraction, we confirmed that the films were epitaxial and the stoichiometry of the films was confirmed using Auger electron spectroscopy. The films have a ferromagnetic Curie temperature (T_C) of 85 ± 5 K and a saturation magnetization of 1 μ_B/Mn. The electric polarization as a function of electric field (*P-E*) was measured using an interdigital capacitance geometry. The *P-E* plot shows a clear hysteresis that confirms the multiferroic nature of the thin films. © *2011 American Institute of Physics*. [doi:10.1063/1.3561860]

I. INTRODUCTION

Multiferroic materials are unique in that they exhibit both ferromagnetism and -electricity simultaneously.[1] Such materials may be used to fabricate devices such as magnetic tunnel junctions with electrically tunable tunneling magnetoresistance and multiple state memory elements.[2] The recent interest in multiferroics is fueled both by the potential device applications and questions about the underlying physical principles leading to multiferroism.[3–7] Bulk multiferroic materials are rare, possibly due to conflicting requirements for ferromagnetism (FM) and ferroelectricity (FE). $BiMnO_3$ is perhaps the most fundamental multiferroic and has been referred to as the "hydrogen atom" of multiferroics.[8] In $BiMnO_3$ (BMO), as in $BiFeO_3$, the $6s^2$ lone pair on the Bi ion leads to the displacement of that ion from the centrosymmetric position at the A-site of a perovskite unit cell. The resultant distortion leads to an FM interaction between the Mn ions at the B-site in BMO.[9,10] In bulk form, BMO has been observed to be both FM and FE.[11] Polycrystalline BMO can be grown under high pressure and within a very narrow range of growth conditions. While thin films of BMO have been grown by various groups, few such films have shown magnetic properties similar to bulk BMO and high enough resistivities, that is, low leakage currents to allow clear measurement of FE properties.[12–14] A possible reason for the low resistivities of BMO thin films is the substrate induced strain, which exacerbates the growth of a highly distorted perovskite structure. Additionally, recent electron and neutron diffraction data have cast doubt over the purported noncentrosymmetry of the BMO crystal structure,[15] and centrosymmetric structures have also been predicted using density functional theory calculations.[16] Because a noncentrosymmetric crystal structure is essential for ferroelectricity, the observed ferroelectric behavior of BMO may be due to strain and/or ordered oxygen vacancies.[17,18]

BMO has a distorted perovskite-type structure with $a = c = 3.935$ Å ($\alpha = \gamma$ 91.4°) and $b = 3.989$ Å ($\beta = 91°$).[19] Figure 1 shows the larger monoclinic unit cell of BMO;[9] we have used the monoclinic notation to index the x-ray diffraction data of our thin films. Because cubic $SrTiO_3$ (STO) has a lattice parameter of 3.905 Å, BMO grows with an 111 orientation on STO 001 substrates under a compressive strain due to a lattice mismatch of 0.77%. It is still unclear whether this strain is responsible for the difference in the magnetic and electrical properties between thin films and polycrystalline BMO. A saturation magnetization M_{sat} of about 3.6 μ_B/Mn at 5 K and a ferromagnetic Curie temperature (T_C) of 105 K have been observed in polycrystalline BMO along with an

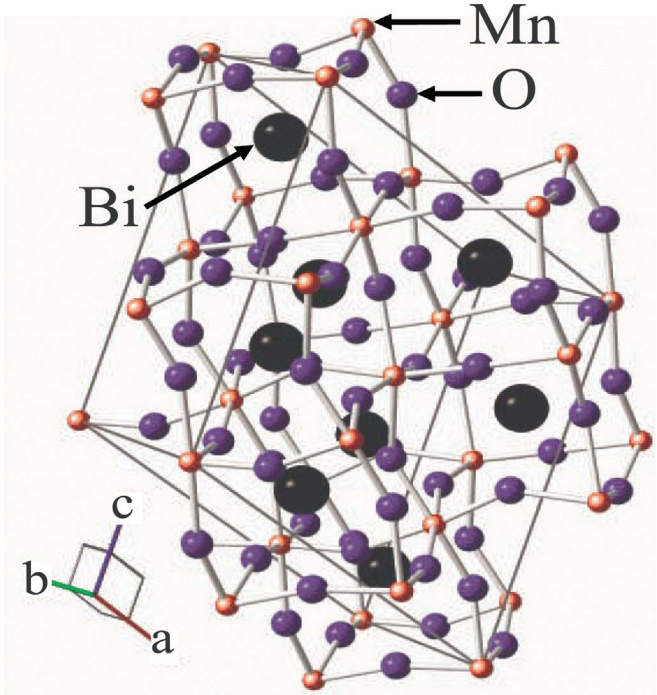

FIG. 1. (Color online) The monoclinic unit cell of $BiMnO_3$. (Ref. 27).

[a]Presently at Department of Physics, University of California, Berkeley, CA 94720, USA and Materials Science Division, Lawrence Berkeley National Laboratory, Berkeley, CA 94720, USA.
[b]Also at Nanoscience Institute of Medical and Engineering Technology, University of Florida, 32611.
[c]Author to whom correspondence should be addressed. Electronic mail: amlan@phys.ufl.edu.

electric remnant polarization of 62 nC/cm^2 at 87 K, while in thin films, an M_{sat} of about 2.2 μ_B/Mn and a T_C of about 100 K have been reported.[11,12,19,20] *P-E* measurements on BMO thin films have been reported occasionally, and a remnant polarization of about 16 μC/cm^2 has been observed.[14] The strain may also influence the ferroelectric domain wall motion, which coupled with the low resistance of the thin films has made it a challenge to confirm the FE nature of BMO thin films leading to the controversial situation presented in the introduction. To address such issues, we have optimized the growth of BMO on STO. We have obtained stoichiometric, epitaxial thin films of BMO that have a high resistivity at low temperature thus facilitating the measurement of *P-E* loops confirming the multiferroic nature of our films.

II. EXPERIMENTAL METHODS

The BMO thin films were grown using pulsed laser deposition (PLD). An off-stoichiometric (Bi-rich) target with composition $Bi_{2.4}MnO_3$ was ablated using a KrF excimer laser ($\lambda = 248$ nm). The high Bi content of the target allowed us to use relatively high substrate temperatures (T_s) and still get the right Bi content for stoichiometric BMO films. The film quality was extremely sensitive to the T_s and the oxygen pressure, and only slightly sensitive to the laser energy, while it was independent of the growth rate within the range used. The laser energy density was kept at 1.0 ± 0.2 J/cm^2. The optimum flowing oxygen pressure and T_s were 37 mTorr and 632 °C, respectively. The film thickness was varied from 30 to 60 nm, and the deposition rate was 0.05 nm/s. The films were cooled in an O_2 atmosphere of 680 Torr at a rate of 20 °C/min (sample type 1) or higher (up to 40 °C/min, sample type 2). The surfaces of the films were imaged using the tapping mode in a Digital Instruments Nanoscope III atomic force microscope (AFM). The structural and chemical properties of the films were characterized with standard θ–2θ x-ray diffraction using a Philips APD 3720 system and Auger electron spectroscopy (AES) using a Perkin-Elmer PHI 660 scanning Auger multiprobe instrument. The magnetization was measured using a Quantum Design SQUID magnetometer. We also measured the electrical polarization using an interdigital capacitance geometry and a Precision LC ferroelectric tester from Radiant Technologies. Here we present results from two 60 nm-thick BMO thin films (one each of sample type 1 and 2). We obtained similar results from the other thin films in the thickness range of 30 to 60 nm.

III. RESULTS AND DISCUSSION

Figure 2(a) shows the x-ray diffraction data for a 60-nm-thick BMO thin film (sample type 1). The inset shows that the BMO grows with a 111 orientation as expected from the structure of BMO. We also observed a small peak corresponding to Mn_2O_3 impurities that is visible in the semilog plot [Fig. 2(b)] (integrated intensity ratio of the Mn_2O_3 peak to the $BiMnO_3$ 111 peak is 0.025). To remove these impurities, we increased the post-deposition cooling rate of T_s to about 40 °C/min in an O_2 atmosphere of 680 Torr. Figure 2(b) also shows the x-ray data for a 60 nm film grown using

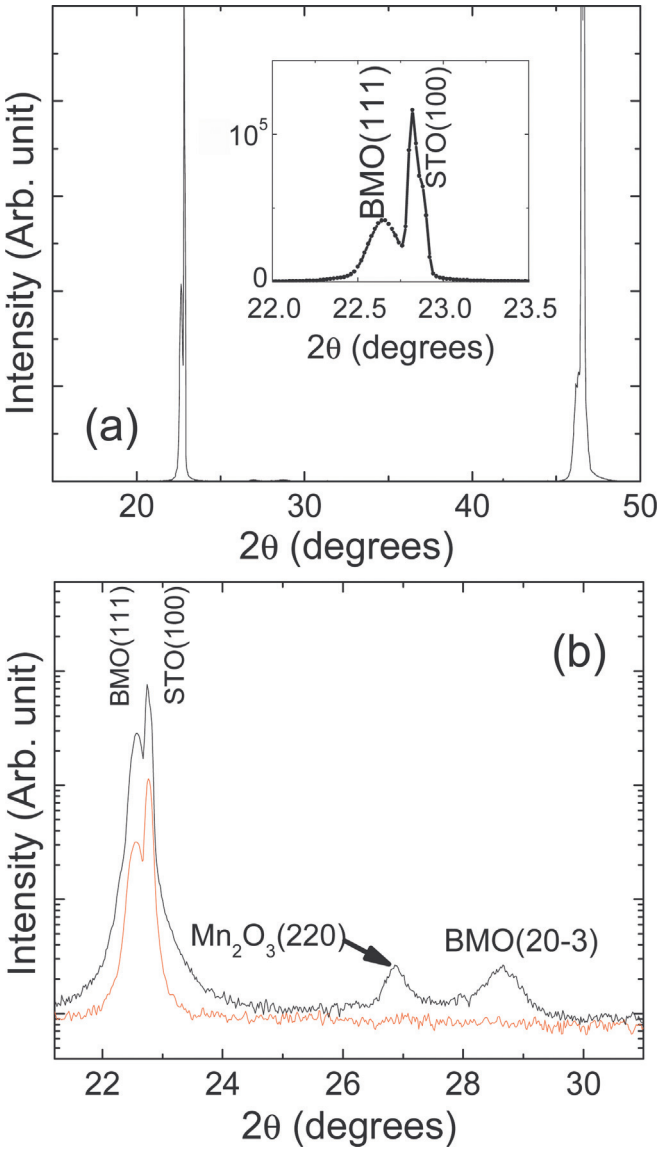

FIG. 2. (Color online) (a) θ–2θ x-ray diffraction pattern of a 60-nm-thick $BiMnO_3$ thin film. The inset shows the $BiMnO_3$ (111) peak in detail. (b) A semilog plot showing a small amount of Mn_2O_3 impurity phase and a small BMO($20\bar{3}$) peak (higher intensity line) and the impurity free film grown using the rapid quenching technique (lower intensity line).

the new cooling rate (sample type 2), which confirms that the impurity peaks have been successfully removed using the modified growth conditions. To confirm the stoichiometry of the samples, we performed Auger electron spectroscopy (AES) measurements at 300 K in ultra high vacuum (UHV) conditions. Derivative AES surface spectra were taken using 5 keV primary electron beam from kinetic energies of 50 to 1500 eV at incident angles from 30 to 60°. Depth profiling was performed by taking surface spectra with the parameters given above followed by an *in situ* repeated 3 keV Ar-ion sputtering. Surface spectra of the BMO films displayed three manganese (Mn) peaks located at 548, 595, and 645 eV, two bismuth (Bi) peaks at 106 and 254 eV and one oxygen (O) peak at 518 eV together with residue carbon (C) peak at 273 eV with concentrations less than 1%. After 6 s of Ar sputtering on the surface, the C peak disappeared and Bi, Mn, and O concentrations are found to be 23.3, 24.1, and 52.6%,

respectively, with about a 2% error. These concentrations imply that the $BiMnO_3$ stoichiometry is consistent with the measured BMO x-ray peaks from θ to 2θ measurements. Moreover, the sensitivity factor for oxygen is based on an MgO matrix, and because there is no matrix parameter in the atomic percentage calculations, this could account for the slightly lower than stoichiometric oxygen concentrations.

The magnetic properties of BMO are closely related to its unique crystal structure. BMO is similar to the compound $LaMnO_3$ (LMO) but due to the 6*s* lone pair, the Bi ion moves away from the centrosymmetric position at the B-site of a perovskite structure. LMO is an A-type antiferromagnet due to antiferromagnetically stacked ferromagnetic layers.[21] In BMO, the distortion caused by the Bi ion leads to an FM interaction between the layers.[9,10] Hence, BMO has an overall magnetic moment that has been measured to be as high as 3.6 μ_B/Mn in polycrystalline samples; this is close to maximum possible magnetization of 4 μ_B/Mn.[19] In thin films, the magnetic moment is reduced quite likely due to the substrate induced strain. The T_C in thin films is also lower than the value of about 105 K obtained in polycrystalline samples.[11,19] Figure 3 shows the *M-T* and *M-H* curves of 60 nm BMO thin films (sample types 1 and 2). The magnetic field was applied in the plane of the film for the magnetic measurements. The *M-T* plot reveals a T_C of about 85 ± 5 K for both sample types. Saturation magnetizations of about 1.0 and 1.1 μ_B/Mn were obtained at 10 K in a field of 50 kOe for sample types 1 and 2, respectively. The inset of Fig. 3(b) shows the hysteresis in the *M-H* plot at different temperatures for sample type 2. A coercive field of about 270 Oe is observed at 10 K, which drops to about 30 Oe at 50 K. The hysteresis of the *M-H* curves and the magnetic moment become negligible at about 80 K, which is close to the estimated T_C, confirming that the observed magnetization is associated with magnetic ordering that happens at a temperature lower than the corresponding T_C of bulk BMO.[11] The reduced magnetic moment of our thin films compared to bulk BMO is not due to the presence of the nonmagnetic impurities because both the sample types 1 and 2 have similar saturation magnetizations and coercive fields. The inset of Fig. 3(a) also shows the surface morphology of sample type 2. Both type 1 and 2 thin films show three-dimensional (3-D) island growth mode with an r.m.s roughness of about 10 nm. It has been shown that 3-D island growth leads to nonuniform strain resulting in high values of strains at the island edges.[22,23] Because the structure of BMO is closely related to that of antiferromagnetic LMO, the nonuniform strain distribution could be responsible for both the reduced values of T_C and saturation magnetization.

A low leakage current and hence high resistivity is a requirement for polarization versus electric field (*P-E*) measurements in BMO thin films. Our optimized thin films have a room temperature resistivity of about 10 Ω-cm, which is lower than values reported by other groups.[6,13] However, by 140 K (below 140 K the resistance is too high to measure with our instrumentation), the resistivity increases to about 1 MΩ-cm, and it was possible to make direct polarization versus electric field (*P-E*) measurements at temperatures below 100 K using an interdigital capacitance geometry [Fig. 4(a)]. The capacitor

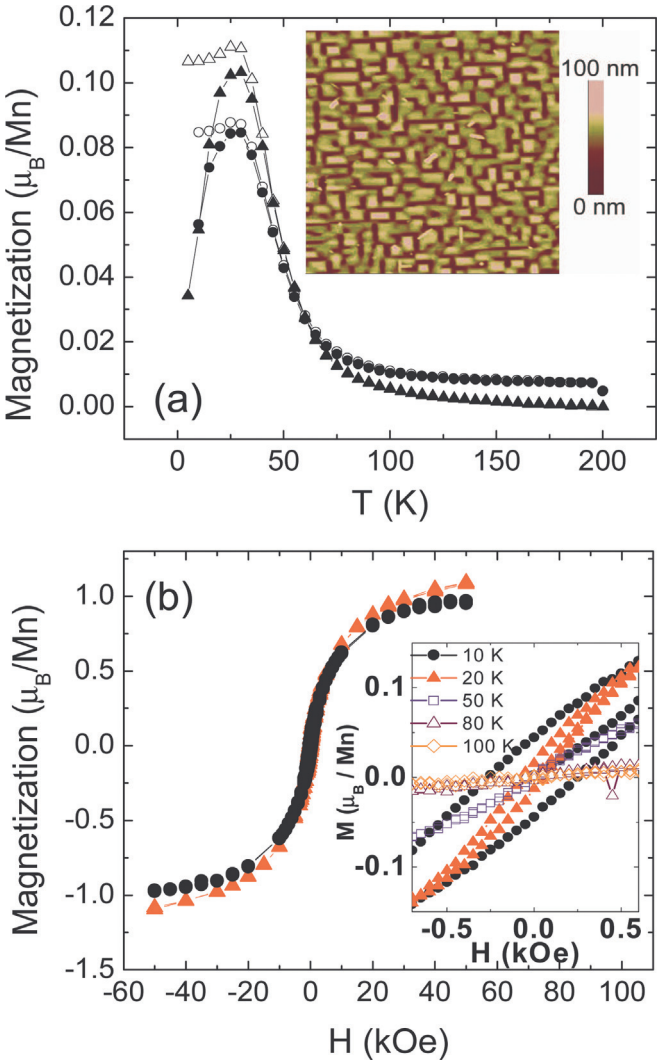

FIG. 3. (Color online) (a) Magnetization vs temperature (*M-T*) plot for two 60-nm-thick $BiMnO_3$ thin films in an in-plane field of 500 Oe, sample 1 (circles) and sample 2 (triangles). The full symbols and open symbols are the zero field cooled and field cooled data respectively. The inset shows a 5×5 μm atomic force microscope image of the surface of sample 2. (b) Magnetization vs magnetic field (*M-H*) plot for sample 1 (circle) and sample 2 (triangle) at 10 K. The inset shows the reduction in the hysteresis of the *M-H* data for sample 2 as the temperature is increased.

is composed of alternating *V*+/*V*− electrodes uniformly spaced on the film surface [Fig. 4(b)]. This structure leads to equipotential planes intersecting the film between each pair of electrodes, resulting in a capacitance between the projected areas of each electrode within the film. The projected areas were calculated using conformal mapping and equating the capacitor thickness to half the electrode spatial wavelength ($\lambda_e = 10$ μm).[24] Figure 4(c) shows the remnant hysteresis loops for a sample type 1 thin film at 5, 55, and 85 K (similar results were obtained for the sample type 2 thin film). The polarization in a hysteresis loop is calculated by integrating the total transferred charge during application of a bipolar triangular voltage waveform. This polarization includes contributions from leakage current, capacitance, and ferroelectric domain switching. The polarization in the remnant hysteresis loop is calculated by isolating the transferred charge from only the domain-switching. This is done by subtracting two

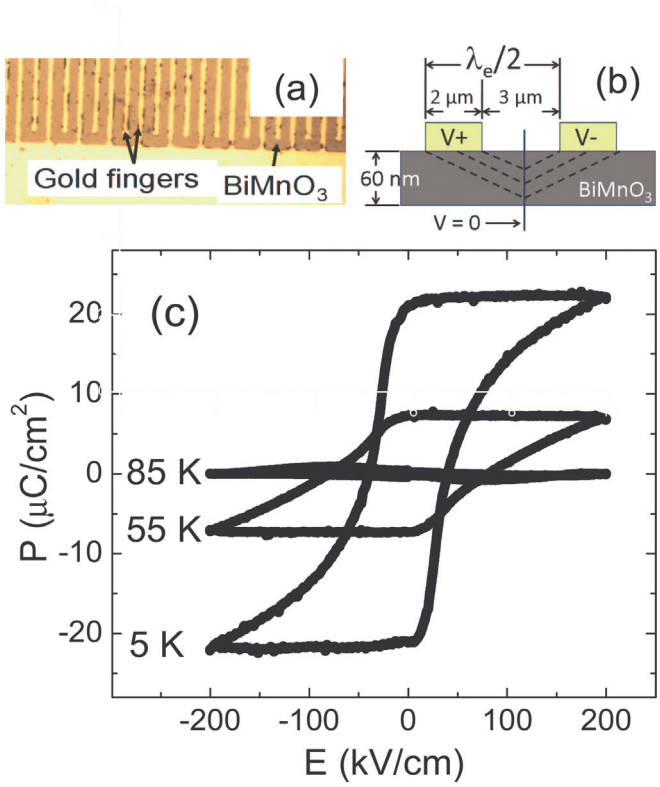

FIG. 4. (Color online) (a) The interdigital capacitance geometry deposited on the film surface. (b) Schematic of the electrode configuration for the *P-E* measurements. (c) Remnant polarization vs. electric field (*P-E*) data of a 60-nm-thick $BiMnO_3$ thin film (sample 1) at three different temperatures.

hysteresis loops that are preceded by poling pulses. In one loop, all of the domains are preswitched so that no domain-switching charge is transferred during the loop, and in the other loop, all the domains are set unswitched with charge transfer from domain-switching beginning at the coercive field. The leakage current and capacitance contributions from the two loops cancel, leaving only transferred charge from domain-switching, or equivalently, the remnant charge. Dividing the remnant charge by the projected area we find a remnant polarization of $P \approx 23\ \mu C/cm^2$ at 5 K, with a coercive field $E_C \approx 40$ kV/cm.

The clear observation of a ferroelectric *P-E* loop appears to be in conflict with the centrosymmetric structure suggested by Belik *et al.*[15] If the crystal structure of BMO is indeed centrosymmetric, then the possible reasons for the ferroelectric behavior of BMO thin films are:[1] structural distortions due to oxygen vacancies,[2,15] a centrosymmetric to noncentrosymmetric transition below T_C that is, below 100 K,[3,15] and substrate induced strain.[17] Although, the AES measurements on our thin films reveal an oxygen deficiency that could lead to the ferroelectric behavior, we cannot rule out the role of substrate induced strain. If the film is uniformly strained, the lattice mismatch, which is −0.77% (compressive), is not enough to break the centrosymmetry as shown by Hatt *et al.*[17] However, it has been shown that compressive lattice mismatch strain could lead to a nonunifrom strain distribution in the thin film due to island formation and the strain at the island edges could far exceed the average lattice mismatch strain.[22,23] The growth morphology of our thin films [inset Fig. 3(a)] suggests that such nonuniform strain distribution is also a possible mechanism for the appearance of ferroelectricity. In addition, because we measured the *P-E* loops at 5 K, the ferroelectric behavior could be due to a structural change below T_C. To test this hypothesis, we have measured the temperature dependence of the *P-E* loops as the temperature is increased above T_C. Figure 4(c) shows that the remnant polarization goes to zero at approximately 85 K, which is close to the ferromagnetic T_C. Hence, the ferroelectricity in BMO thin films appears to be related to their magnetism. The correlation of magnetism and ferroelectricity is possibly due to the nonuniform strain distribution, which results in inhomogeneous magnetism and leads to breaking of inversion symmetry.[25]

IV. CONCLUSIONS

In summary, we have grown impurity free thin films of $BiMnO_3$ 111 on $SrTiO_3$ 001 substrates. The films have the desired structure and stoichiometry. The ferromagnetic T_C is 85 ± 5 K with a saturation magnetization of about 1 μ_B/Mn at 10 K. The films have a sufficiently high resistivity at low temperatures to allow the measurement of *P-E* loops. A remnant polarization of 23 $\mu C/cm^2$ was measured at 5 K with a coercive field of 40 kV/cm. Nonuniform strain distribution may be responsible for the reduced T_C, reduced saturation magnetization, and the appearance of ferroelectricity in these BMO thin films. Hence, strain dependent measurements of the magnetic and electrical properties are necessary to reveal the origin of multiferroism in BMO.[26]

ACKNOWLEDGMENTS

This work was supported by NSF DMR-0804452 (A.B.) and NSF DMR-1005301 (A.F.H.).

[1]H. Schmid, Ferroelectrics **162**, 317 (1994).
[2]M. Gajek, M. Bibes, S. Fusil, K. Bouzehouane, J. Fontcuberta, A. Barthelemy, and A. Fert, Nat. Mater. **6**, 296 (2007).
[3]N. A. Spaldin and M. Fiebig, Science **309**, 391 (2005).
[4]C. N. R. Rao and C. R. Serrao, J. Mater. Chem. **17**, 4931 (2007).
[5]M. Fiebig, J. Phys. D **38**, R123 (2005).
[6]W. Eerenstein, N. D. Mathur, and J. F. Scott, Nature **442**, 759 (2006).
[7]W. Prellier, M. P. Singh, and P. Murugavel, J. Phys.: Condens. Mat. **17**, 7753 (2005).
[8]N. A. Hill and K. M. Rabe, Phys. Rev. B **59**, 8759 (1999).
[9]T. Atou, H. Chiba, K. Ohoyama, Y. Yamaguchi, and Y. Syono, J. Solid State Chem. **145**, 639 (1999).
[10]A. M. dos Santos, A. K. Cheetham, T. Atou, Y. Syono, Y. Yamaguchi, K. Ohoyama, H. Chiba, and C. N. R. Rao, Phys. Rev. B **66**, 064425 (2002).
[11]A. M. dos Santos, S. Parashar, A. R. Raju, Y. S. Zhao, A. K. Cheetham, and C. N. R. Rao, Solid State Commun. **122**, 49 (2002).
[12]W. Eerenstein, F. D. Morrison, J. F. Scott, and N. D. Mathur, Appl. Phys. Lett. **87**, 101906 (2005).
[13]M. Gajek, M. Bibes, A. Barthelemy, K. Bouzehouane, S. Fusil, M. Varela, J. Fontcuberta, and A. Fert, Phys. Rev. B **72**, 020406 (2005).
[14]J. Y. Son and Y.-H. Shin, Appl. Phys. Lett. **93**, 062902 (2008).
[15]A. A. Belik, S. Iikubo, T. Yokosawa, K. Kodama, N. Igawa, S. Shamoto, M. Azuma, M. Takano, K. Kimoto, Y. Matsui, and E. Takayama-Muromachi, J. Am. Chem. Soc. **129**, 971 (2007).
[16]P. Baettig, R. Seshadri, and N. A. Spaldin, J. Am. Chem. Soc. **129**, 9854 (2007).
[17]A. J. Hatt and N. A. Spaldin, Eur. Phys. J. B **71**, 435 (2009).
[18]H. Yang, Z. H. Chi, J. L. Jiang, W. J. Feng, J. F. Dai, C. Q. Jin, and R. C. Yu, J. Mater. Sci. **43**, 3604 (2008).

[19]H. Chiba, T. Atou, and Y. Syono, J. Solid State Chem. **132**, 139 (1997).
[20]A. F. M. dos Santos, A. K. Cheetham, W. Tian, X. Q. Pan, Y. F. Jia, N. J. Murphy, J. Lettieri, and D. G. Schlom, Appl. Phys. Lett. **84**, 91 (2004).
[21]J. B. Goodenough, Phys. Rev. **100**, 564 (1955).
[22]A. Biswas, M. Rajeswari, R. C. Srivastava, Y. H. Li, T. Venkatesan, R. L. Greene, and A. J. Millis, Phys. Rev. B **61**, 9665 (2000).
[23]Y. Chen and J. Washburn, Phys. Rev. Lett. **77**, 4046 (1996).
[24]R. Igreja and C. J. Dias, Sens. Actuator, A **112**, 291 (2004).
[25]S.-W. Cheong and M. Mostovoy, Nat. Mater. **6**, 13 (2007).
[26]J. Tosado, T. Dhakal, and A. Biswas, J. Phys.: Condens. Mat. **21**, 192203 (2009).
[27]T. C. Ozawa and S. J. Kang, J. Appl. Cryst. **37**, 679 (2004).